

Cytotoxicity and mechanism of action of a new ROS-generating microsphere formulation for circumventing multidrug resistance in breast cancer cells

Qun Liu · Adam Shuhendler · Ji Cheng ·
Andrew Michael Rauth · Peter O'Brien ·
Xiao Yu Wu

Received: 1 May 2009 / Accepted: 7 July 2009 / Published online: 18 July 2009
© Springer Science+Business Media, LLC. 2009

Abstract Multidrug resistance (MDR) is one of the main challenges in the treatment of breast cancer. A new microsphere formulation able to generate reactive oxygen species (ROS) locally was thus investigated for circumventing MDR in breast cancer cells in this work. Glucose oxidase (GOX) was encapsulated in alginate/chitosan hydrogel microspheres (ACMS-GOX). The *in vitro* cytotoxicity of ACMS-GOX to murine breast cancer EMT6/AR1.0 cells, which overexpress P-glycoprotein (P-gp), was evaluated by a clonogenic assay. The mechanism of the cytotoxicity of ACMS-GOX was investigated by using various extracellular and intracellular ROS scavengers and antioxidant enzyme inhibitors. The effect of lipid peroxidation and cellular uptake of GOX was also evaluated. ACMS-GOX exhibited similar dose and time-dependent cytotoxicity to EMT6/AR1.0 cells as to their wild-type EMT6/WT parent cells, in effect circumventing the MDR phenotype of EMT6/AR1.0 cells. Extracellular H₂O₂ and intracellular hydroxyl radical were found to play critical roles in the cytotoxicity of ACMS-GOX. Cellular uptake of GOX was negligible and thus not responsible for intracellular ROS generation. Combining ACMS-GOX with intracellular antioxidant inhibitors-enhanced cytotoxicity. This work demonstrates that the ACMS-GOX are effective in circumventing P-gp-mediated MDR in breast cancer cells.

Keywords Multidrug resistance · Breast cancer · Reactive oxygen species · Microspheres · Cytotoxicity

Introduction

Multidrug resistance (MDR) can develop in tumor cells as a result of chronic exposure to nontoxic levels of a therapeutic agent and clinically may be one of the main reasons for the failure of systemic chemotherapy [1]. Cellular-based MDR generally results from the overexpression of protein transporters located in the cell membrane. These transporters belong to the adenosine triphosphate (ATP)-binding cassette (ABC) family, e.g., P-glycoprotein (P-gp), MDR-associated protein (MRP), lung resistance protein (LRP), and breast cancer-related protein (BCRP) [2]. They serve as energy-dependent drug efflux pumps, exporting a wide range of structurally and functionally unrelated anti-cancer agents out of cells. Directly inhibiting these transporters, as a way of overcoming MDR, has been extensively investigated for more than two decades [3, 4]. However, the relatively high toxicity of the first and second generation P-gp inhibitors, e.g., verapamil and cyclosporine A, has led to the exploration of a third generation of P-gp inhibitors, such as valspodar, which shows lower toxicity, higher affinity to P-gp (or other MDR transporters), and better pharmacokinetic behavior. Nevertheless, these inhibitors are still in clinical trial.

The difficulties encountered in attempting to overcome MDR by directly inhibiting cell membrane transporters have prompted alternate approaches based on the study of molecular mechanisms regulating MDR transporter expression. These approaches have focused on either inhibiting gene expression of MDR transporters in more efficient ways or circumventing the MDR mechanism.

Q. Liu · A. Shuhendler · J. Cheng · P. O'Brien · X. Y. Wu (✉)
Leslie Dan Faculty of Pharmacy, University of Toronto, 144
College Street, Toronto, ON M5S 3M2, Canada
e-mail: xywu@phm.utoronto.ca

A. M. Rauth
Division of Experimental Therapeutics, Ontario Cancer Institute,
610 University Avenue, Toronto, ON M5G 2M9, Canada

Examples of the former approach include the down-regulation of MDR transporter genes, e.g. *mdr1* gene, using anti-sense oligonucleotides, ribozymes, small interfering RNAs (siRNAs), and short hairpin RNA (shRNA) [5], and of the latter, the use of drugs that are poor substrates for MDR transporters such as the anthracyclines idarubicin and anamycin [6].

Elevated reactive oxygen species (ROS) levels have been reported to down-regulate expression of the multidrug resistance type 1 (*mdr1*) gene, which encodes P-gp [7], suggesting that the MDR phenotype can be circumvented by a modest increase of intracellular ROS generation [8, 9]. In addition, ROS are not substrates for MDR transporters and therefore could circumvent the MDR effect. In fact, it has been reported that bovine serum amine oxidase (BSAO) is more toxic to MDR cancer cells than to its wild-type counterpart by producing ROS, suggesting that the MDR cells are sensitive to ROS [10, 11].

ROS, including hydrogen peroxide (H_2O_2), superoxide anion ($\bullet O_2^-$), and hydroxyl radical ($\bullet OH$), are by-products of normal cellular metabolism that directly affect cellular functions, e.g. development, growth, and aging. A moderate level of intracellular ROS is thought to be essential to maintain an appropriate redox balance and to stimulate cellular proliferation [12]. On the other hand, excessive production of ROS can result in detrimental cellular damage including lipid peroxidation, protein oxidation, and DNA adduct formation, which can all ultimately lead to cell death via apoptosis or necrosis [13, 14]. The cytotoxicity of some anticancer agents has been attributed, at least partially, to increased intracellular ROS levels. For example, the anthracycline family, such as doxorubicin (Dox) and daunorubicin, induced apoptosis by increasing intracellular ROS [15, 16].

Among ROS, H_2O_2 has been shown to induce apoptosis of many tumor cells in vitro [17–19]. However, H_2O_2 was ineffective when it was injected alone into the tumors or into the circulation due to its rapid clearance and to its decomposition by catalase in erythrocytes [20, 21]. Several in situ H_2O_2 -generating enzymes, such as glucose oxidase (GOX) [22, 23], BSAO [24–26], amino acid oxidase [27], and xanthine oxidase [28], have been evaluated as alternate approaches to deliver H_2O_2 to solid tumors. The antitumor activity of these enzymes has been demonstrated both in vitro and in vivo. However, the free enzyme is rapidly degraded or cleared by the host when administered systemically. Daily intraperitoneal administration of GOX was required to inhibit tumor growth [22]. In order to increase GOX stability, it has been conjugated to polyethylene glycol (PEG), but repeated intratumoral administration of PEG-GOX was needed to achieve in vivo toxicity [23].

Locoregional delivery of therapeutic agents to solid tumors by microspheres or nanoparticles can increase the

local concentration and extend the residence time of the encapsulated drugs due to their continuous release. This approach has shown promising results with higher efficacy and decreased systemic toxicity compared to systemic drug administration [29–35]. Our laboratory has successfully developed dextran-based microspheres for the local delivery of Dox and MDR reversal agents to solid tumors resulting in significant delays in tumor growth [32, 33]. With new solid polymer-lipid nanoparticle formulations, greatly enhanced uptake, retention, and cytotoxicity of Dox in MDR breast cancer cells in vitro were obtained [36, 37]. To develop a microsphere formulation for in situ production of ROS inside solid tumor, we have encapsulated GOX in alginate/chitosan hydrogel microspheres (ACMS-GOX) and demonstrated well-maintained enzymatic activity [38]. The ability of ACMS-GOX to produce hydrogen peroxide was equivalent or superior to that of free GOX (FR-GOX) at longer times (after 3 h). The ability to produce ROS in situ for a prolonged time is desirable for local treatment of solid tumors without frequently repeated injections.

Based on previous research by various groups including our laboratory, the present work focused on the investigation into a novel strategy of circumventing rather than directly inhibiting the MDR mechanism of drug resistant cancer cells using the ROS-generating enzyme, GOX. The cytotoxicity of free GOX and ACMS-GOX against murine MDR EMT6/AR1.0 breast cancer cells and their wild-type counterpart EMT6/WT cells was examined using a clonogenic assay. To delineate the site of enzymatic action, i.e., inside or outside the microsphere, GOX release from the ACMS-GOX was tested. To characterize whether free GOX or GOX released from ACMS-GOX can enter the cells, fluorescence-labeled GOX was prepared, and its cellular uptake was examined. The mechanism of the cytotoxicity of ACMS-GOX was investigated by the use of extracellular ROS scavengers and intracellular antioxidant enzyme inhibitors.

Materials and methods

Materials

Cell culture medium, alpha-minimal essential medium (α -MEM) plus antibiotics (streptomycin and penicillin, 0.1 g/l each), was obtained from the Ontario Cancer Institute Media Supply Service (Toronto, ON, Canada). Fetal bovine serum (FBS) was from Cansera International Inc. (Etobicoke, ON, Canada). All cell culture plastic wares were supplied by Sarstedt (Montreal, Que, Canada). PeroXOquantTM quantitative peroxide assay kit (aqueous compatible formulation) was purchased from Pierce (Rockford, IL, USA). Catalase (CAT), superoxide dismutase (SOD),

deferoxamine mesylate (DEF), 3-amino-1,2,4-triazole (3-AT), L-buthionine-(S,R)-sulfoxine (BSO), diethyldithiocarbamate (DDC), ciclopirox olamine (CIC), alginate (sodium salt, medium molecular weight, viscosity of 2.0% solution, 25°C, 3,500 cps), and glucose oxidase (Type X-S, 190 U/mg, from *Aspergillus niger*) were all obtained from Sigma (St. Louis, MO, USA). Chitosan was from Fluka (Buchs, SG, Switzerland) and modified before use as previously described [39].

Preparation of ACMS and GOX loading into ACMS

ACMS were prepared as described previously [38]. Briefly, 20 mg of calcium carbonate was added to 6.0 ml of 1.5% (w/v) sodium alginate solution and placed in an ultrasonic bath (VWR, West Chester, PA, USA) for 4 min. The suspension was dispersed into 30 ml of light mineral oil containing 1.5% (v/v) of Span 80 and 0.2% (v/v) of acetic acid at a stirring speed of 760 rpm at room temperature. Next, 120 ml of distilled deionized (DDI) water was added to the above emulsion. Stirring continued for 40 min at a speed of 300 rpm. The calcium alginate (CaAlg) gel beads were separated, rinsed, and subjected to GOX loading.

In a typical GOX loading experiment, 0.5 ml of CaAlg gel beads was added into 0.5 ml of 0.2 mg/ml GOX in a buffer solution (0.2 M, pH 4 (KHC₆H₄(COO)₂-HCl)). The adsorption experiments were carried out for 30 min at 4°C. Then, 1% (w/v) of chitosan acetic acid solution (1%, v/v) was added for 10 min to coat the CaAlg gel beads. The concentration of GOX in the solution before and after loading and coating was characterized by the BioRad (Hercules, CA, USA) protein microassay. The percentage of GOX loading and encapsulation efficiency were calculated using the following equations:

$$\text{GOX loading} = \frac{\text{weight of GOX loaded}}{\text{weight of total particles}} \times 100\%$$

$$\text{Encapsulation efficiency} = \frac{\text{weight of GOX loaded}}{\text{total weight of GOX added to the preparation}} \times 100\%.$$

GOX release and ACMS swelling test

The GOX release test was carried out using 0.5 ml of ACMS-GOX (3.5 mg dry weight) in 10 ml of 0.2 M pH 6.0 and pH 7.4 (KH₂PO₄-NaOH) buffer solutions at 37°C. The concentration of GOX in the buffer solution was measured by the BioRad (Hercules, CA, USA) protein

microassay. Briefly, an 800 µl-sample was taken at different time intervals, 200 µl of assay solution was added, the mixture was incubated at room temperature for 10 min, and the ultraviolet (UV) adsorption of the mixture at 596 nm was measured. After each sampling, an 800 µl of the fresh buffer was added to the testing medium.

The swelling measurements of ACMS-GOX were carried out at 0.2 M pH 6.0 or pH 7.4 buffer solution (KH₂PO₄-NaOH) as well. Around 5 µl of ACMS-GOX was added to 100 µl of buffer solution on the glass slide. The size change of ACMS was observed under a microscope (LEITZ DM IL, Leica, Wetzlar, Germany). At different time intervals, from 1 to 30 min, pictures were taken with a digital camera (Canon A75, Canon, Tokyo, Japan). The diameters of 10 selected beads in each picture were then measured on a computer using Universal Desktop Ruler software (AVPSoft). The swelling ratio was defined as the volume after swelling divided by the original volume of ACMS.

Determination of kinetics of H₂O₂ generation

The kinetics of H₂O₂ generation by ACMS-GOX was determined by a PeroXOquantTM quantitative peroxide assay kit (Pierce, Rockford, IL, USA). ACMS-GOX, 0.5 ml (3.95 mg of dry weight), loaded at different concentrations of GOX (0.4, 2, 10 U/ml) were incubated in 10 ml of culture medium in a humidified incubator at 37°C. At different time intervals, an 800 µl aliquot of the culture medium (as defined below) was taken and centrifuged for 1 min using Centricon YM-50 (Millipore, Billerica, MA, USA) with a cutoff molecular weight of 50,000 kDa. To 20 µl of filtrate, 200 µl of the assay kit was added. The mixture was incubated for 15 min at room temperature, and then its absorbance was measured at 595 nm using a microplate reader (Molecular Device, Sunnyvale, CA, USA).

Cell lines and cell cultures

Parent EMT6/WT murine breast carcinoma cells and its MDR derivative EMT6/AR1.0 cells, which overexpress P-gp, were generously provided by Dr. I. F. Tannock of the Ontario Cancer Institute (Toronto, ON, Canada). The doubling time of the cell lines during the exponential growth phase was 14–16 h. Cells (5–30 passages in our hands) were cultured as a monolayer on 75-cm² tissue culture flasks in α-MEM plus antibiotics (streptomycin and penicillin, 0.1 g/l each) supplemented with 10% FBS (defined as culture medium) in a 5% CO₂/95% air humidified incubator at 37°C. Confluent cultures were trypsinized with 0.05% trypsin-EDTA (Invitrogen, Burlington, ON, Canada) and subcultured twice a week.

Evaluation of the cytotoxicity of FR-GOX and ACMS-GOX

All the in vitro cytotoxicity experiments were carried out using cells grown as a monolayer in a humidified incubator with 5% CO₂/95% air at 37°C. Twenty-four hours prior to treatment, 5×10^5 cells were seeded in 10-cm petri dishes containing 10 ml of growth medium. For the drug treatment experiments, aliquots of ACMS-GOX loaded with equivalent doses of free GOX (FR-GOX) were incubated with EMT6/WT or EMT6/AR1.0 cells for 1 h, respectively. Following incubation, cells were rinsed and trypsinized and assayed for survival using a clonogenic assay. Cells without GOX treatment were run as a control. The cytotoxicity of blank ACMS was also evaluated on both cell lines for 5 h exposures. For EMT6/AR1.0 cells, the cytotoxicity of ACMS-GOX with exposure times of 1, 3, and 5 h was also examined.

Determination of cellular uptake of GOX

GOX was conjugated to fluorescein isothiocyanate (FITC-GOX) using an EZ-labelTM fluorescein protein labeling kit (Pierce, Rockford, IL, USA) and loaded into ACMS microspheres as described earlier. The microencapsulated or free FITC-GOX were incubated with wild-type or drug-resistant EMT6 cells, 1×10^5 cells per well seeded 24 h earlier in a 96-well plate, for 0, 1, 3, and 5 h. After incubation, the cells were washed three times with cold PBS and assayed for uptake of FITC-GOX on a fluorescence plate reader (Molecular Device, Sunnyvale, CA, USA).

Clonogenic assay

A clonogenic assay was employed to determine the cytotoxicity of different treatments. After the treatments, the cells were rinsed with 5 ml of PBS three times and then trypsinized. The resuspended cells were counted with a hemocytometer and plated at various dilutions (100, 1,000, 10,000) in duplicate in 6-cm petri dishes containing 5 ml of growth medium. The cultures were incubated for 6–7 days allowing viable cells to grow into macroscopic colonies. Then, the medium was removed, and the cells were fixed and stained with a 0.5% solution of methylene blue in 50% ethanol. The number of colonies formed was counted on a light table, from which plating efficiencies were determined by the number of colonies formed divided by the number of cells plated in the culture dishes. Relative surviving fractions were then calculated by dividing the plating efficiency of the drug-treated cells by that of the cells without treatment [40]. The control plating efficiencies of EMT6/WT and EMT6/AR1.0 were 0.54 ± 0.12 and 0.48 ± 0.10 ($n = 10$), respectively.

Determination of lipid peroxidation of cells caused by GOX

To determine the mechanism of the cytotoxicity, the extent of lipid peroxidation was determined by following the evolution of thiobarbituric acid-reactive substances. EMT6/AR1.0 and EMT6/WT cells were seeded in 10-cm plastic petri dishes at 1×10^6 cells per dish in 10 ml of growth medium for 24 h. The cells were then treated with FR-GOX or ACMS-GOX for 0, 1, 3, and 5 h, after which time the cells were scraped free of the dish surface using a rubber policeman. A 2 ml aliquot of cell suspension was combined with 2 ml of 70% trichloroacetic acid and mixed well. Then, 2 ml of thiobarbituric acid was added, and the mixture was boiled for 5 min. The solutions were centrifuged, and the supernatants were read on a UV/Vis spectrophotometer (Agilent Technologies, Santa Clara, CA, USA) at 540 nm.

Evaluation of the cytotoxicity in the presence of extracellular ROS scavengers and intracellular antioxidant enzyme inhibitors

In an attempt to identify which species of ROS play essential roles in GOX-induced cytotoxicity as well as to determine whether they act extracellularly or intracellularly, the cytotoxicity of ACMS-GOX was evaluated following treatment with extracellular ROS scavengers and intracellular antioxidant enzyme inhibitors. To test the effect of extracellular ROS, CAT, SOD, and the iron chelator DEF were used to reduce extracellular H₂O₂, [•]O₂, and [•]OH, respectively. Cultured cells were incubated with ACMS-GOX together with CAT (2,000 U/ml), SOD (300 U/ml), or DEF (1 mM) for 1 h, respectively [41]. To assess the effect of intracellular ROS, cultured cells were preincubated with the intracellular catalase inhibitor 3-AT (20 mM for 2 h), the glutathione (GSH) peroxidase synthesis inhibitor BSO (5 mM for 22 h), the SOD inhibitor DDC (1 mM for 1 h), or an intracellular iron chelator CIC (0.1 mM for 15 min), respectively. Cells without treatment, treatment with ACMS-GOX only, and treatment with the individual ROS scavenger and antioxidant enzyme inhibitor were run as controls. Following incubation, cells were rinsed, trypsinized, and the cytotoxicity evaluated using the clonogenic assay, as described previously.

Statistical analysis

All the cytotoxicity experiments were repeated at least three times. Two-sided Student's *t*-test was applied to compare the cytotoxicity of different treatments of ACMS-GOX to the cells. A value of $P < 0.05$ was considered statistically significant.

Results

Kinetics of GOX release and ACMS swelling as a function of pH

The local pH in solid tumors can be as acidic as pH 6.0 owing to the formation and accumulation of lactic acid. Therefore, the leakage test of GOX from ACMS and swelling behavior of ACMS were evaluated at normal physiologic pH 7.4 and pH 6.0. As shown in Fig. 1a, in the pH 7.4 buffer solution no detectable amount of GOX was released from ACMS within 8 h. In the pH 6.0 buffer solution, less than 3% of GOX was released in 1 h, and around 20% was released in 8 h. A slight increase in the swelling ratio to about 1.2 was observed in the pH 7.4 buffer solution, whereas there was no change in swelling ratio in pH 6.0 buffer (Fig. 1b). These results suggest that the leakage of GOX is not related to swelling and might be due to GOX loosely bound onto the surface of the ACMS. The ACMS remained spherical in shape after the swelling experiment.

Kinetics of H₂O₂ generation

Figure 2 illustrates that the H₂O₂ generation is proportional to the concentration of GOX in ACMS-GOX at the exposure times of 1, 3, and 5 h, respectively. With a dose of 400 mU/ml of GOX in ACMS-GOX, the concentration of H₂O₂ reached 0.38 mM at 1 h and increased 4.4 fold to 1.68 mM at 5 h. The pH of the culture medium dropped to around 7.2 from 7.4 due to the transformation of glucose to gluconic acid by the catalytic action of ACMS-GOX.

In vitro cytotoxicity of ACMS-GOX to EMT6/WT and EMT6/AR1.0

Figure 3 compares the surviving fraction of EMT6/AR1.0 and EMT6/WT after 1 h exposure at 37°C to the increasing doses of ACMS-GOX or FR-GOX. The dose-dependent cytotoxicity curves for both cell lines are very close, indicating complete avoidance of the MDR defense in the resistant cells by the ACMS-GOX (Fig. 3a). The same phenomenon is also observed in the FR-GOX-treated cells (Fig. 3b). The blank ACMS with an equivalent mass of microspheres as ACMS-GOX exhibited no effect on the surviving fraction of either wild-type or drug-resistant cells after incubation for up to 5 h (data not shown), indicating that blank ACMS are not toxic to the cells under the test conditions. The cytotoxicity of FR-GOX was 4–6 times greater than an equivalent amount of ACMS-GOX.

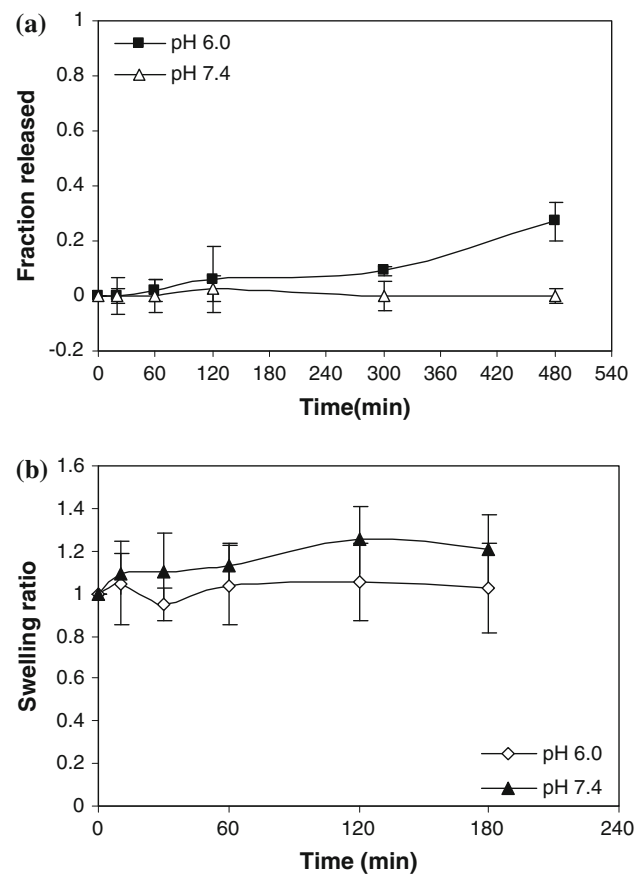


Fig. 1 Kinetics of **a** GOX release from the ACMS at 37°C and **b** ACMS swelling at room temperature in a 0.2 M, pH 6.0 or pH 7.4 KH₂PO₄-NaOH buffer solution. The ACMS-GOX were prepared, unless otherwise specified, by incubating CaAlg gel beads (dry weight of 3.95 mg) in 0.5 ml of 1.0 mg/ml GOX in 0.2 M buffer solution of pH 4 and then coated with 1% (w/v) chitosan solution. The data points and error bars represent mean \pm SD of triplicate experiments; where not shown, the SD values lie within the symbols

Effect of exposure time and concentration of H₂O₂ on the cytotoxicity of ACMS-GOX toward EMT6/AR1.0 cells

Figure 4a presents the surviving fraction of EMT6/AR1.0 cells as a function of time of exposure (1, 3, and 5 h) to different GOX doses in the form of ACMS-GOX or for 1-h exposure of FR-GOX. A dependence of the cytotoxicity on exposure time of ACMS-GOX is demonstrated. The dose for 90% cell killing is about 360, 280, and 180 mU/ml at exposure times of 1, 3, and 5 h, respectively. As the exposure time increases from 1 to 5 h, the survival curves for ACMS-GOX become steeper, approaching the curve for FR-GOX with 1-h exposure. However, to achieve equivalent cell killing as FR-GOX, even a longer exposure time is required.

The form of the time-dependent cytotoxicity curves of ACMS-GOX may be ascribed to the rate of H₂O₂

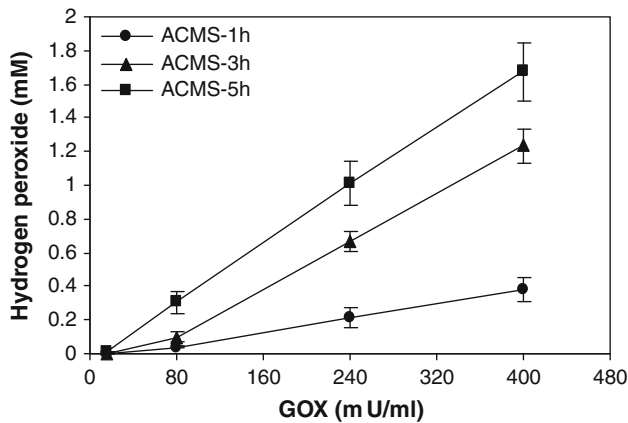


Fig. 2 Hydrogen peroxide generation by ACMS-GOX in culture medium as a function of GOX dose and reaction time. About 0.5 ml of ACMS-GOX (3.95 mg of dry weight), loaded with different concentrations of GOX (0.4, 2, 10 U/ml), were incubated in 10 ml of culture medium in a humidified incubator at 37°C for 1, 3, or 5 h. The data points and the error bars represent mean \pm SD ($n = 3$); where not seen, the SD values lie within the symbols

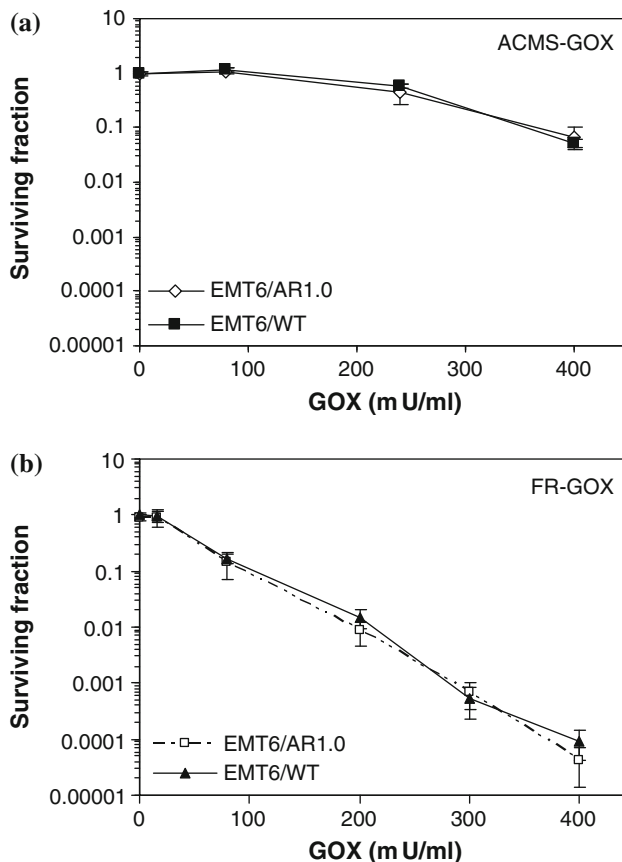


Fig. 3 Comparison of surviving fractions of EMT6/WT and EMT6/AR1.0 cells treated for 1 h with different doses of **a** ACMS-GOX or **b** FR-GOX. About 5×10^5 cells were seeded in 10-cm petri dishes containing 10 ml of growth medium 24 h before the treatment. The data points and error bars represent mean \pm SD of at least three independent experiments, where not shown, the SD values lie within the symbols

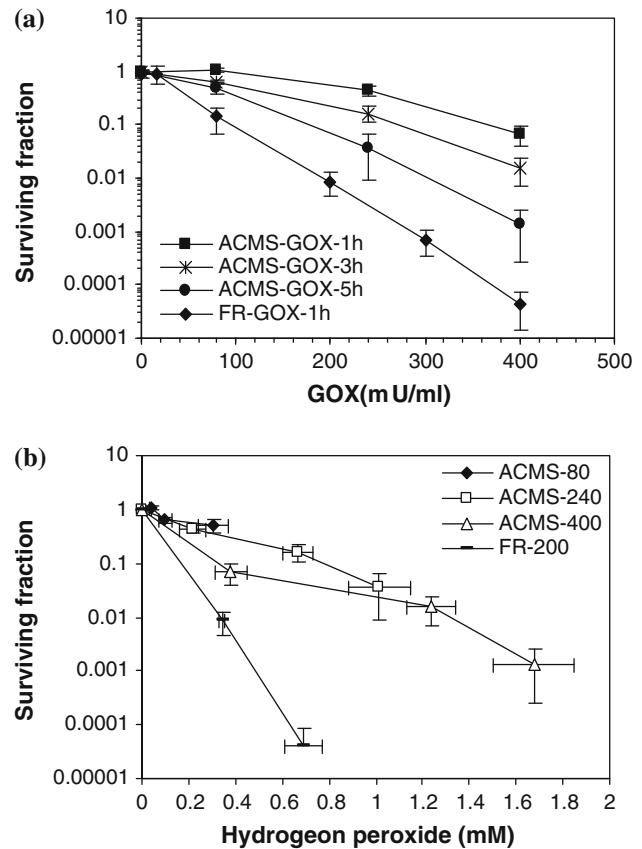


Fig. 4 Cytotoxicity of ACMS-GOX or FR-GOX to EMT6/AR1.0 cells as measured by cell colony forming ability (survival fraction) **a** with various doses of ACMS-GOX for 1, 3, or 5 h exposures or FR-GOX for 1-h exposures. About 5×10^5 cells were seeded in 10-cm petri dishes containing 10 ml of growth medium 24 h before the treatment. The data points and error bars represent mean \pm SD of at least three independent experiments. Where not shown, the SD values lie within the symbols. **b** The data from panel **a** have been replotted using the data from Fig. 2, this article, for H₂O₂ generation from ACMS-GOX and data from [35] for H₂O₂ generation from FR-GOX for comparison. Error bars indicate standard errors of the mean for three or more determinations

production, which is slower than FR-GOX as reported previously [38]. To analyze whether H₂O₂ concentration at various times generated by different formulations would be a contributing factor, the H₂O₂ concentration was measured in separate experiments (the kinetics of H₂O₂ generation as indicated in Fig. 2). Figure 4b illustrates the relationship between cytotoxicity and H₂O₂ concentration as generated from ACMS-GOX and FR-GOX. In each curve, different data points represent different levels of H₂O₂ produced (1, 3, and 5 h for ACMS-GOX and total treatment of 5 h; and 1 and 3 h for FR-GOX, total treatment of 3 h). For ACMS-GOX, 1.68, 1.01, and 0.31 mM of H₂O₂ was generated, corresponding to doses of 400, 240, and 80 mU/ml within a 5 h time period. As a result, surviving fractions of 0.001, 0.037, and 0.504 were obtained.

Table 1 Cytotoxicity of ACMS-GOX to EMT6/AR1.0 cells with different cell density

	Control	Cell density (10^6 cells)		
		0.5	1	2
Surviving fraction	1.00 \pm 0.04	0.03 \pm 0.03	0.31 \pm 0.03*	0.68 \pm 0.11*

Treatment was performed by treating 0.5, 1, and 2 millions of cells seeded 24 h before the treatment in 10-cm petri dishes with ACMS-GOX at an equivalence dose of 400 mU/ml for 1 h. The values represent mean \pm SD of three independent experiments

Bold values denote the surviving fraction as indicated in the most left column (e.g. 1 means 100%, 0.03 means 3% and so forth)

* The significant difference between 1 and 2 millions of cells treatment group compared with that of 0.5 millions of cells treatment group, $P < 0.001$

For FR-GOX, 0.689 mM of H_2O_2 was generated in 3 h, corresponding to a surviving fraction of 3.92×10^{-5} . Apparently, the dose dependence of cytotoxicity for ACMS-GOX is consistent with the curves from different exposure times falling in the close vicinity. Nevertheless, the dose–response curve for FR-GOX is much steeper, suggesting that other factors may play a role in the cytotoxicity besides the level of hydrogen peroxide generated.

Effect of cell density on the cytotoxicity of ACMS-GOX to EMT6/AR1.0 cells

Previous work has indicated cell density-dependent cytotoxicity of anticancer drugs [2, 42]. Hence, a study was undertaken to find out whether cell density would affect the in vitro efficacy of ACMS-GOX. Table 1 shows that as the number of EMT6/AR1.0 cells seeded 24 h before treatment increases from 0.5 to 2 million, the cytotoxicity of ACMS-GOX containing 400 mU/ml GOX equivalent decreased dramatically from approximately 97% to 32% cell killing for 1-h exposure to ACMS-GOX.

Lipid peroxidation of EMT6/AR1.0 cells treated with FR-GOX and ACMS-GOX

Over a time course of 5 h, FR-GOX and ACMS-GOX at a dose of 80 mU/ml were found to induce lipid peroxidation in both cell lines (data not shown). The degree of peroxidation was higher in EMT6/AR1.0 cells than in EMT6/WT cells when treated with FR-GOX for various times and when treated with ACMS-GOX for 5 h. The result suggested that the MDR cells were more susceptible to ROS-induced cellular damage than the wild-type cells. A higher degree of lipid peroxidation was observed in cells treated with FR-GOX than with ACMS-GOX, attributable to the more rapid production of H_2O_2 by FR-GOX compared to ACMS-GOX.

Cellular uptake of GOX

To see whether the difference in the cytotoxicity between FR-GOX and ACMS-GOX is caused by cellular uptake of GOX, FITC-GOX was prepared, and its intracellular levels were measured with a fluorescence plate reader. The results indicated no detectable FITC-GOX in either EMT6/WT or EMT6/AR1.0 cells (data not shown). Hence, the possibility that FR-GOX enters the cells more readily thus causing higher cytotoxicity was excluded.

In vitro cytotoxicity of ACMS-GOX in the presence of extracellular ROS scavengers and intracellular antioxidant enzyme inhibitors

In order to identify which ROS play critical roles in the cytotoxicity of GOX toward EMT6/AR1.0 cells and whether the free radicals act extracellularly or intracellularly, the modulation of the cytotoxicity of ACMS-GOX by extracellular ROS scavengers and intracellular antioxidant enzyme inhibitors was evaluated by measuring cell colony forming ability. As illustrated in Fig. 5a, a 1-h exposure to catalase by itself at 2,000 U/ml was nontoxic to cells and, in fact, increased the survival of EMT6/AR1.0 cells by approximately 40%. SOD alone at 300 U/ml did not affect the viability of the cells significantly after a 1-h exposure, and DEF at 1 mM for 1 h by itself exhibited minor cytotoxicity to the cells. Figure 5b reveals that catalase totally inhibited the cytotoxicity of 1-h exposures to both ACMS-GOX (400 mU/ml) and FR-GOX (80 mU/ml), whereas SOD completely inhibited the cytotoxicity of FR-GOX, but only slightly reduced the cytotoxicity of the ACMS-GOX. The ferric chelator DEF marginally inhibited the cytotoxicity of both ACMS-GOX and FR-GOX.

The preincubation of cells with intracellular antioxidant enzyme inhibitors 3-AT, BSO, DDC, or CIC at the concentrations and times tested reduced cell survival by themselves to 70–90% of the control EMT6/AR1.0 cells as demonstrated in Fig. 6a. Preincubation and the presence of the antioxidant enzyme inhibitors 3-AT, BSO, and DDC enhanced the cytotoxicity of 1-h exposure to ACMS-GOX (400 mU/ml) to EMT6/AR1.0 cells, while CIC significantly reduced the cytotoxicity of ACMS-GOX as shown in Fig. 6b.

Discussion

H_2O_2 release locally from ACMS-GOX

One of the major obstacles for systemic chemotherapy is the low concentration of antineoplastic agents available in the local tumor tissue to elicit extensive cell killing.

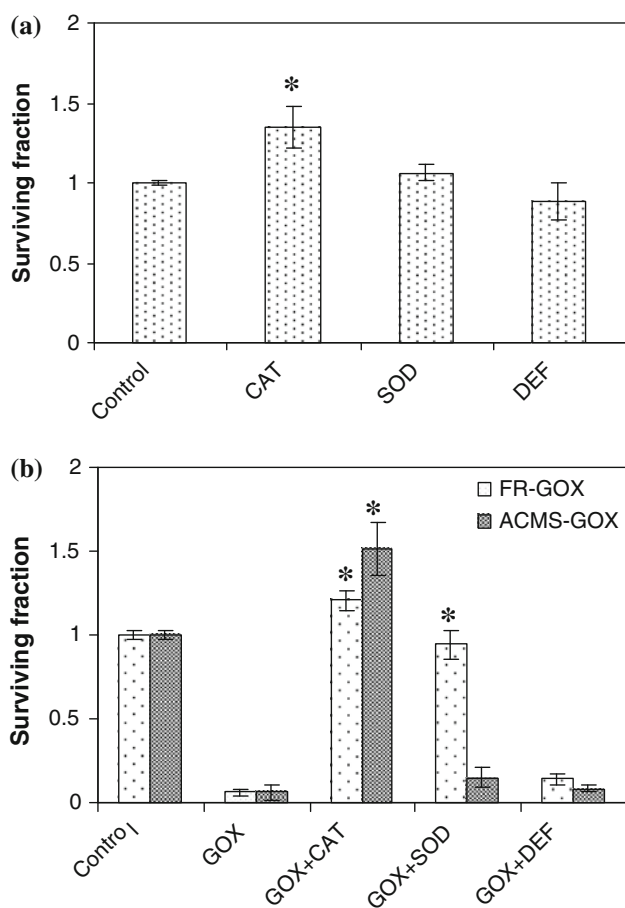


Fig. 5 Cytotoxicity of ACMS-GOX to EMT6/AR1.0 in the presence of extracellular-free radical scavengers CAT, SOD, and DEF. About 5×10^5 cells were seeded in 10-cm petri dishes containing 10 ml of growth medium 24 h before the treatment. **a** Surviving fraction of cells without treatment, treatment with CAT (2,000 U/ml), SOD (300 U/ml), or DEF (1 mM) for 1 h, respectively. **b** Control cells and cells treated with ACMS-GOX (400 mU/ml) or FR-GOX (80 mU/ml) only, with ACMS-GOX or FR-GOX together with CAT (2,000 U/ml), SOD (300 U/ml), or DEF (1 mM) for 1 h, respectively. The *data points* and *error bars* represent mean \pm SD of at least three independent experiments, where not shown, the SD values lie within the *symbols*. * Indicates the significant difference in different treatment groups compared to the control (**a**) or to the GOX treatment group (**b**), $P < 0.001$

Previous results of local delivery of antineoplastic agents encapsulated in micro/nanoparticles from our laboratory have shown promising results with enhanced therapeutic effect for solid tumor treatment [33, 43]. Furthermore, GOX was encapsulated and stabilized in polysaccharide-based alginate/chitosan particles, which was effective for EMT6/WT cells [44]. Free H_2O_2 is not effective for tumor treatment because it is unstable and easily degraded in vivo. Thus, the alternative approach of using H_2O_2 -generating enzymes has been investigated for cancer treatment. However, systemic administration of these enzymes might be expected to exhibit systemic cytotoxicity similar to

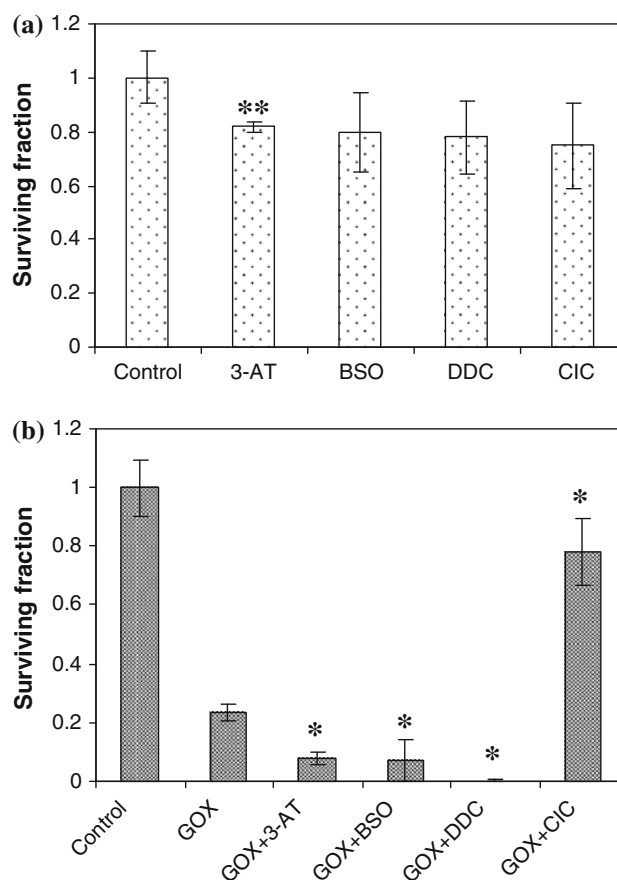


Fig. 6 Cytotoxicity (surviving fraction) of ACMS-GOX to EMT6/AR1.0 in the presence of intracellular antioxidant enzyme inhibitors. About 5×10^5 cells were seeded in 10-cm petri dishes containing 10 ml of growth medium 24 h before the treatment. Cultured cells were preincubated with intracellular catalase inhibitor 3-AT (20 mM for 2 h), glutathione (*GSH*) peroxidase inhibitor BSO (5 mM for 22 h), SOD inhibitor DDC (1 mM for 1 h), or an intracellular ferric chelator CIC (0.1 mM for 15 min), respectively. **a** Cells without GOX treatment but treatment with individual intracellular antioxidant enzyme inhibitors were run as controls. **b** Control cells or cells treated with ACMS-GOX (400 mU/ml for 1 h) or cells pretreated with the individual antioxidant enzyme inhibitors and ACMS-GOX. The *data points* and *error bars* represent mean \pm SD of at least three independent experiments, where not shown, the SD values lie within the *symbols*. * Indicates the significant difference in different treatments compared to the GOX treatment group, $P < 0.05$ for GOX + CIC treatment group; $P < 0.001$ for the other treatment groups. ** Indicates the significant difference between treatment and control group, $P < 0.05$

conventional anticancer agents [23]. Thus, local delivery of ACMS-GOX to tumors to generate H_2O_2 could provide a safer way, with less systemic side effects, to elevate local ROS concentrations in the tumor tissue. In the current work, GOX was shown to remain in the ACMS, and no burst release was observed. The continuous generation of H_2O_2 from ACMS-GOX could act as a depot for the release of ROS locally to the tumor tissue. For the 1-h exposures tested in the present work, the mechanism of

cytotoxicity induced by ACMS-GOX was assuredly from bound GOX, not from released free GOX (Fig. 1).

Locally released H_2O_2 from ACMS-GOX bypassed MDR mechanism

Interestingly, ACMS-GOX exhibited similar time and dose-dependent cytotoxicity to MDR EMT6/AR1.0 cells with overexpression of P-gp as their parent EMT6/WT cells (Fig. 3). This indicates that ACMS-GOX can efficiently kill the MDR cells without inhibition by P-gp. The development of the MDR phenotype is often associated with the overexpression of membrane transporters, e.g., P-gp, which act as an energy-dependent drug efflux pumps exporting various anticancer drugs out of cells. The cells might acquire cellular-based MDR by chronic exposure of cancer cells to a nontoxic level of anticancer drugs. The results shown in the present study suggest that H_2O_2 generated by ACMS-GOX can bypass the P-gp transporter to induce similar cytotoxicity to MDR cells as to wild-type cells. This is because the cytotoxicity of GOX was mediated by the generation of H_2O_2 , which is not a substrate of P-gp. H_2O_2 readily crosses the cell membrane [24]. Diffusion of extracellularly generated H_2O_2 into the cells can cause increased H_2O_2 levels intracellularly, which are toxic to the cells if the concentration is beyond the capacity of detoxification of antioxidant enzymes, such as catalase, glutathione peroxidase and SOD.

In fact, increased ROS levels have been observed in cancer cells compared to more normal cells due to their fast proliferation and enhanced metabolic rate. MDR cells exhibit even higher ROS levels than their wild-type counterparts due to the increased energy required for elevated mitochondrial activity for the overexpression of membrane transporters [45]. Therefore, MDR cells might be more sensitive to an additional increase in ROS levels compared to non-MDR cells. In the current work, MDR type EMT6/AR1.0 cells showed more lipid peroxidation by extracellular generation of ROS than their wild-type counterpart. This is probably due to enhanced intracellular ROS levels of MDR cells. Cytotoxicity of BASO caused by the generation of H_2O_2 has been shown to be more toxic to MDR cells than wild-type cells [10, 11]. In addition, the lipid peroxidation level was in agreement with the H_2O_2 generation profile suggesting that lipid peroxidation was directly affected by H_2O_2 concentration generated by GOX. Free GOX produced H_2O_2 more rapidly thus causing more damage. ACMS-GOX produced higher H_2O_2 concentrations more gradually than FR-GOX; hence, more lipid peroxidation occurred at 5 h in EMT6/AR1.0 cells.

The dose for killing the same fraction of EMT6/AR1.0 cells for ACMS-GOX was around 3.6-fold greater than that for FR-GOX at the 0.1% survival level (Fig. 4). This is

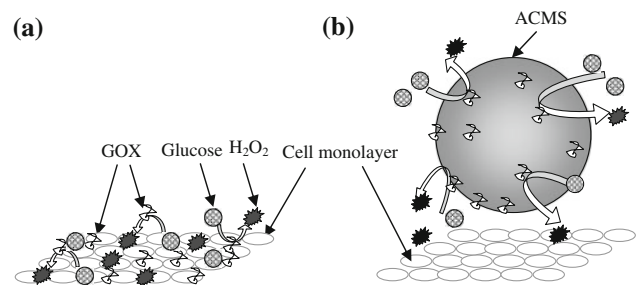


Fig. 7 Schematic illustration of the mechanism of the cytotoxicity of **a** FR-GOX, which is distributed evenly and adjacently to the cells, allowing the H_2O_2 generated to directly diffuse into the cells; **b** ACMS-GOX, which is located in multiple discrete spots in the cell culture dishes floating on the top of the cell monolayer. The H_2O_2 generated needs to diffuse out of the microspheres, travel to the cells, and then cross the cell membranes

probably due to the difference in the site of ROS generation and diffusion distance of H_2O_2 in these two systems as depicted in Fig. 7. FR-GOX is distributed evenly and adjacently to the cells, allowing the H_2O_2 generated to directly diffuse into the cells. However, ACMS-GOX are located in multiple discrete spots in the cell culture dishes, floating on the top of the cell monolayer. The H_2O_2 generated needs to diffuse out of the microspheres, travel to the cells, and then cross the cell membranes. Another reason for the reduced efficacy of ACMS-GOX compared to FR-GOX could be the lower generation rate of H_2O_2 by ACMS-GOX (Fig. 4b) due to steric hindrance and enzyme rigidification after encapsulation of GOX into ACMS, which lowers the efficacy of enzyme and substrate binding. In addition, the substrate, glucose, has easier access to FR-GOX than ACMS-GOX. At a lower generation rate, the antioxidant enzymes in the cells can decompose the generated ROS more effectively. However, ACMS-GOX showed time-dependent cytotoxicity to the cells. Therefore, the advantage of ACMS-GOX is its enhanced stability over FR-GOX, allowing for its application as a long-term treatment. The cytotoxicity of H_2O_2 was dependent on the number of cells that were treated (Table 1), indicating that the decomposition of H_2O_2 by cellular enzymes or enhanced reaction sites for H_2O_2 could dilute out the reactive species with an increased number of sites for the ROS to react with.

Mechanism of the cytotoxicity of ACMS-GOX

H_2O_2 readily crosses cellular membranes and causes oxidative damage to DNA, proteins, and lipids by direct oxidation or via the transition metal-driven Haber–Weiss reaction, which is initiated by the Fenton reaction, and results in the extremely reactive $\cdot OH$ [46–48].

In the current study, to assess whether the cytotoxicity induced by ACMS-GOX was a direct result of H_2O_2 or

mediated by other toxic oxygen metabolites, several extracellular reactive oxygen metabolites scavengers (CAT for H_2O_2 , SOD for $\cdot\text{O}_2^-$, and DEF for preventing the formation of $\cdot\text{OH}$ by removing iron) were examined (Fig. 5). Catalase completely prevented the cytotoxicity, however, only a marginal effect was observed when SOD or DEF was present, respectively. This suggests that the cytotoxicity of ACMS-GOX to EMT6/AR1.0 cells was mediated by H_2O_2 extracellularly. Although some H_2O_2 can be transformed into highly reactive $\cdot\text{OH}$ extracellularly, $\cdot\text{OH}$ was not effective extracellularly due to its short half-life (10^{-9} s) and short diffusion radius (2.3 nm) [49]. This is consistent with a previous study of oligodendrocytes in which the iron chelator, DEF, had no effect on H_2O_2 cytotoxicity [50]. One possible explanation may be a direct attack on membrane lipids by H_2O_2 . CAT depletion of H_2O_2 before it can act on the cells might be the most efficacious defense against H_2O_2 -induced cytotoxicity [51]. At the same time, part of H_2O_2 generated extracellularly diffuses into cells. H_2O_2 could be transformed to $\cdot\text{OH}$, which is far more reactive than $\cdot\text{O}_2^-$ and H_2O_2 , as $\cdot\text{OH}$ reacts indiscriminately with the closest neighboring molecules [46]. The remarkable protection of cells afforded by CIC against oxidative stress indicated that intracellular cytotoxicity of ACMS-GOX was mediated through highly reactive $\cdot\text{OH}$ (Fig. 6). As an extremely reactive-free radical, $\cdot\text{OH}$ attacks all biological molecules. However, due to the short half-life and diffusion radius, $\cdot\text{OH}$ could only cause cytotoxicity intracellularly. Therefore, intracellular cytotoxicity was mainly mediated by highly reactive $\cdot\text{OH}$ instead of H_2O_2 . In summary, the cytotoxicity of ACMS-GOX was induced both extracellularly and intracellularly.

Conclusions

A novel strategy of using the ROS-generating enzyme GOX immobilized in ACMS to continuously generate H_2O_2 for treatment of MDR cancer cells with P-gp overexpression was investigated. GOX appeared to be stably incorporated into the ACMS without a burst release effect. ACMS-GOX exhibited similar cytotoxicity to MDR EMT6/AR1.0 cells like its wild-type parent cells, indicating the ACMS-GOX effectively circumvents P-gp transporter. The greater cytotoxicity induced into MDR cells with longer incubation resulted from the accumulation of the continuously released H_2O_2 from immobilized GOX. This could be an advantage of ACMS-GOX over FR-GOX for extended treatments. H_2O_2 generated extracellularly played an essential role in tumor cell killing, while the intracellular cytotoxicity seemed to depend on the Fenton-mediated conversion of H_2O_2 to $\cdot\text{OH}$. These results also demonstrate that the treatment of ACMS-GOX in

combination with intracellular antioxidant enzyme inhibitors could enhance the cytotoxicity of ACMS-GOX to the tumor cells.

Acknowledgments The authors sincerely thank Dr. P. Wells for allowing them to use their cell culture facilities, Dr. T. Preston, Ms. C. Lee, and Ms. A. Ramkissoon for their kind help and useful discussion. The University of Toronto Open Fellowships and Ben Cohen Fund conferred to Q. Liu, the Ontario Graduate Scholarship and University to up-fund to A. Shuhendler are also gratefully acknowledged.

References

1. Wong HL, Wu XY, Bendayan R (2009) Multidrug resistance in solid tumor and its reversal. In Lu Y, Mahato RI (eds.) *Pharmaceutical aspects of cancer chemotherapy (on invitation)*. Springer, New York, pp. 121–148.
2. Tannock IF, Hill RP (1998) *The basic science of oncology*. In: Tannock IF, Goldenberg GJ (eds) *Drug resistance and experimental chemotherapy*. McGraw-Hill, Toronto, pp 392–419
3. McDevitt CA, Callaghan R (2007) How can we best use structural information on P-glycoprotein to design inhibitors? *Pharmacol Ther* 113:429–441
4. Leonard GD, Polgar O, Bates SE (2002) ABC transporters and inhibitors: new targets, new agents. *Curr Opin Investig Drugs* 3:1652–1659
5. Lage H (2006) MDR1/P-glycoprotein (ABCB1) as target for RNA interference-mediated reversal of multidrug resistance. *Curr Drug Targets* 7:813–821
6. Liscovitch M, Lavie Y (2002) Cancer multidrug resistance: a review of recent drug discovery research. *Drugs* 5:349–355
7. Ziemann C, Burkle A et al (1999) Reactive oxygen species participate in mdrlb mRNA and P-glycoprotein overexpression in primary rat hepatocyte cultures. *Carcinogenesis* 20:407–414
8. Wartenberg M, Hoffmann E et al (2005) Reactive oxygen species-linked regulation of the multidrug resistance transporter P-glycoprotein in Nox-1 overexpressing prostate tumor spheroids. *FEBS Lett* 579:4541–4549
9. Wartenberg M, Ling FC et al (2001) Down-regulation of intrinsic P-glycoprotein expression in multicellular prostate tumor spheroids by reactive oxygen species. *J Biol Chem* 276:17420–17428
10. Calcabrini A, Arancia G et al (2002) Enzymatic oxidation products of spermine induce greater cytotoxic effects on human multidrug-resistant colon carcinoma cells (LoVo) than on their wild-type counterparts. *Int J Cancer* 99:43–52
11. Lord-Fontaine S, Agostinelli E et al (2001) Amine oxidase, spermine, and hyperthermia induce cytotoxicity in P-glycoprotein overexpressing multidrug resistant Chinese hamster ovary cells. *Biochem Cell Biol* 79:165–175
12. McCord JM (1995) Superoxide radical: controversies, contradictions, and paradoxes. *Proc Soc Exp Biol Med* 209:112–117
13. Hampton MB, Fadeel B, Orrenius S (1998) Redox regulation of the caspases during apoptosis. *Ann N Y Acad Sci* 854:328–335
14. Hileman EO, Liu J et al (2004) Intrinsic oxidative stress in cancer cells: a biochemical basis for therapeutic selectivity. *Cancer Chemother Pharmacol* 53:209–219
15. Ravi D, Das KC (2004) Redox-cycling of anthracyclines by thioredoxin system: increased superoxide generation and DNA damage. *Cancer Chemother Pharmacol* 54:449–458
16. Kotamraju S, Konorev EA et al (2000) Doxorubicin-induced apoptosis in endothelial cells and cardiomyocytes is ameliorated by nitron spin traps and ebselen. Role of reactive oxygen and nitrogen species. *J Biol Chem* 275:33585–33592

17. Kim DS, Jeon SE et al (2006) Hydrogen peroxide is a mediator of indole-3-acetic acid/horseradish peroxidase-induced apoptosis. *FEBS Lett* 580:1439–1446
18. Poh TW, Pervaiz S (2005) LY294002 and LY303511 sensitize tumor cells to drug-induced apoptosis via intracellular hydrogen peroxide production independent of the phosphoinositide 3-kinase-Akt pathway. *Cancer Res* 65:6264–6274
19. Ren JG, Xia HL et al (2001) Hydroxyl radical-induced apoptosis in human tumor cells is associated with telomere shortening but not telomerase inhibition and caspase activation. *FEBS Lett* 488:123–132
20. Green HN, Westrop JW (1958) Hydrogen peroxide and tumor therapy. *Nature* 181:128–129
21. Mealey J (1965) Regional infusion of vinblastine and hydrogen peroxide in tumor-bearing rats. *J Cancer Res* 25:1839–1843
22. Higuchi Y, Shoin S, Matsukawa S (1991) Enhancement of the antitumor effect of glucose oxidase by combined administration of hydrogen peroxide decomposition inhibitors together with an oxygenated fluorocarbon. *Jpn J Cancer Res* 82:942–949
23. Ben-Yoseph O, Ross BD (1994) Oxidation therapy: the use of a reactive oxygen species-generating enzyme system for tumour treatment. *Br J Cancer* 70:1131–1135
24. Averill-Bates DA, Cherif A et al (2005) Anti-tumoral effect of native and immobilized bovine serum amine oxidase in a mouse melanoma model. *Biochem Pharmacol* 69:1693–1704
25. Demers N, Agostinelli E et al (2001) Immobilization of native and poly(ethylene glycol)-treated ('PEGylated') bovine serum amine oxidase into a biocompatible hydrogel. *Biotechnol Appl Biochem* 33:201–207
26. Arancia G, Calcabrini A et al (2004) Mitochondrial alterations induced by serum amine oxidase and spermine on human multidrug resistant tumor cells. *Amino Acids* 26:273–282
27. Fang J, Sawa T et al (2002) Tumor-targeted delivery of polyethylene glycol-conjugated D-amino acid oxidase for antitumor therapy via enzymatic generation of hydrogen peroxide. *Cancer Res* 62:3138–3143
28. Sawa T, Wu J et al (2000) Tumor-targeting chemotherapy by a xanthine oxidase-polymer conjugate that generates oxygen-free radicals in tumor tissue. *Cancer Res* 60:666–671
29. Sugiyama T, Kumagai S et al (1998) Experimental and clinical evaluation of cisplatin-containing MS as intraperitoneal chemotherapy for ovarian cancer. *Anticancer Res* 18:2837–2842
30. Tokuda K, Natsugoe S et al (1998) Design and testing of a new cisplatin form using a base material by combining poly-D, L-lactic acid and poly(ethylene glycol) acid against peritoneal metastasis. *Int J Cancer* 76:709–712
31. Hagiwara A, Sakakura C et al (1998) Therapeutic effects of 5-fluorouracil microspheres on peritoneal carcinomatosis induced by Colon 26 or B-16 melanoma in mice. *Anticancer Drugs* 9:287–289
32. Liu Z, Ballinger JR et al (2003) Delivery of an anticancer drug and a chemosensitizer to murine breast sarcoma by intratumoral injection of sulfopropyl dextran microspheres. *J Pharm Pharmacol* 55:1063–1073
33. Cheung RY, Rauth AM, Wu XY (2005) In vivo efficacy and toxicity of intratumorally delivered mitomycin C and its combination with doxorubicin using microsphere formulations. *Anticancer Drugs* 16:423–433
34. Liu J, Meisner D, Kwong E, Wu XY, Johnston MR (2009) Trans-lymphatic delivery of paclitaxel by intrapleural placement of gelatin sponge impregnated with PLGA-paclitaxel microspheres effectively controls lymphatic metastasis in an orthotopic lung cancer model. *Cancer Res* 69:1174–1181
35. Wong HL, Rauth AM, Bendayan R, Wu XY (2007) In vivo evaluation of a new polymer-lipid hybrid nanoparticle (PLN) formulation of doxorubicin in a murine solid tumor model. *Eur J Pharm Biopharm* 65:300–308
36. Wong HL, Rauth AM et al (2006) A new polymer-lipid hybrid nanoparticle system increases cytotoxicity of doxorubicin against multidrug-resistant human breast cancer cells. *Pharm Res* 23:1574–1585
37. Shuhendler AJ, Cheung R, Manias J, Connor A, Rauth AM, Wu XY (2009) A novel doxorubicin-mitomycin C co-encapsulated nanoparticle formulation exhibits anti-cancer synergy in multidrug resistant human breast cancer cells. *Breast Cancer Res Treatment*. doi: 10.1007/s10549-008-0271-3 (Epub Apr 2009)
38. Liu Q, Rauth AM, Wu XY (2007) Immobilization and bioactivity of glucose oxidase in hydrogel microspheres formulated by an emulsification-internal gelation-adsorption-polyelectrolyte coating method. *Int J Pharm* 339:148–156
39. Hsu SC, Don TM, Chiu WY (2002) Free radical degradation of chitosan with potassium persulfate. *Polym Degrad Stab* 75:73–83
40. Bristow RG, Hill RP (1998) The Basic Science of Oncology. In: Tannock IF, Hill RP (eds) *Molecular and cellular basis of radiotherapy*. McGraw-Hill, Toronto, pp 295–321
41. Rollet-Labelle E, Grange MJ et al (1998) Hydroxyl radical as a potential intracellular mediator of polymorphonuclear neutrophil apoptosis. *Free Radic Biol Med* 24:563–572
42. Cheung RY, Rauth AM et al (2006) In vitro toxicity to breast cancer cells of icosphere-delivered mitomycin C and its combination with doxorubicin. *Eur J Pharm Biopharm* 62:321–331
43. Wong HL, Bendayan R et al (2006) A mechanistic study of enhanced doxorubicin uptake and retention in multidrug resistant breast cancer cells using a polymer-lipid hybrid nanoparticle system. *J Pharma Expert Ther* 317:1372–1381
44. Liu Q (2008) Enzyme microencapsulation and its application for overcoming multidrug resistance in breast cancer treatment. University of Toronto, Toronto
45. Pelicano H, Carney D, Huang P (2004) ROS stress in cancer cells and therapeutic implications. *Drug Resist Updat* 7:97–110
46. Beckman KB, Ames BN (1997) Oxidative decay of DNA. *J Biol Chem* 272:19633–19636
47. Berlet BS, Stadtman ER (1997) Protein oxidation in aging, disease, and oxidative stress. *J Biol Chem* 272:20313–20316
48. Halliwell B, Gutteridge JM (1984) Free radicals, lipid peroxidation and cell damage. *Lancet*. 23:1396–1397
49. Roots R, Okada S (1975) Estimation of life times and diffusion distances of radicals involved in X-ray-induced DNA strand breaks or killing of mammalian cells. *Radiat Res* 64:306–320
50. Baud O, Greene AE et al (2004) Glutathione peroxidase-catalase cooperativity is required for resistance to hydrogen peroxide by mature rat oligodendrocytes. *J Neurosci* 24:1531–1540
51. Ohta H, Okamoto I et al (2006) Enhanced antioxidant defense due to extracellular catalase activity in Syrian hamster during arousal from hibernation. *Comp Biochem Physiol C* 143:484–491